Two-dimensional hydrogenated buckled gallium arsenide: an ab initio study

Two-dimensional hydrogenated buckled gallium arsenide: An ab-initio study

Two-dimensional hydrogenated buckled gallium arsenide: An *ab-initio* study

A. González-García[1 2], W. López-Pérez[1], R. González-Hernández[1 4], J. Rivera-Julio[2 3], C. Espejo[1], M. V. Milosevic[2], and F. M. Peeters[2]

[1] Grupo de Investigación en Física Aplicada, Departamento de Física, Universidad del Norte, Barranquilla, Colombia.

[2] Departement Fysica, Universiteit Antwerpen, Groenenborgerlaan 171, B-2020 Antwerpen, Belgium.

[3] Condensed matter theory group, Centro Atomico Bariloche and CONICET, S. C. de Bariloche, 8400 S. C. de Bariloche, Argentina

[4] Institut für Physik, Johannes Gutenberg Universität Mainz, D-55099 Mainz, Germany

E-mail: alvarogonzalez@uninorte.edu.co

Abstract. First-principles calculations have been carried out to investigate the stability, structural and electronic properties of two−dimensional hydrogenated GaAs with three possible geometries: chair, zigzag−line and boat configurations. The effect of van der Waals interactions on 2D H−GaAs systems has also been studied. These configurations were found to be energetic and dynamic stable, as well as having a semiconducting character. Although two−dimensional GaAs adsorbed with H tends to form a zigzag−line configuration, the energy differences between chair, zigzag−line and boat are very small which implies the metastability of the system. Chair and boat configurations display a Γ−Γ direct bandgap nature, while pristine 2D−GaAs and zigzag−line are indirect semiconductors. The bandgap sizes of all configurations are also hydrogen dependent, and wider than that of pristine 2D−GaAs with both PBE and HSE functionals. Even though DFT−vdW interactions increase the adsorption energies and reduce the equilibrium distances of H−GaAs systems, it presents, qualitatively, the same physical results on the stability and electronic properties of our studied systems with PBE functional. According to our results, two−dimensional buckled gallium arsenide is a good candidate to be synthesized by hydrogen surface passivation as its group III−V partners two-dimensional buckled gallium nitride and boron nitride. The hydrogenation of 2D-GaAs tunes the bandgap of pristine 2D-GaAs, which makes it a potential candidate for optoelectronic applications in the blue and violet ranges of the visible electromagnetic spectrum.

Submitted to: *J. Phys.: Condens. Matter*

Keywords:Density Functional Theory, bandgap tuning, hydrogen, two- dimensional gallium arsenide.

1. Introduction

Electronic properties of 2D materials can be tuned by chemical functionalization [1, 2]. When radical atoms are adsorbed on the 2D surface they can form covalent, ionic or van der Waals bonds with the in-plane atoms. These atoms change the 2D-material hybridization from sp^2 to sp^3, which leads to the opening of a bandgap, eg. graphene, a gapless semimetal, becomes a wide bandgap semiconductor when is fully hydrogenated [3]. Furthermore, adsorption of hydrogen on 2D materials modifies their structural, optical, magnetic and mechanical properties [4, 5].

Chemical adsorption of hydrogen atoms on two-dimensional materials generates other new crystals with different geometries. Therefore, new hydrogen-based two-dimensional crystals are built with different physical properties from their pristine parent material. Among the several ordering patterns of adatoms on the pristine 2D-material, the most studied metastable geometries are chair, zigzag-line and boat [2, 4, 6–8]. As shown in Figure 1, in the chair (boat) geometry the hydrogen atoms alternate singly (pairwise) on either side of the GaAs plane, while in the zigzag-line configuration the hydrogen atoms of one hexagon alternate three-up and three-down on the GaAs plane. For the chair configuration the unit cell is hexagonal, while for the other two cases the unit cell is rectangular.

Shu *et al* [4] found that hydrogenated germanene tends to form chair and zigzag-line configurations, where its electronic and optical properties show close geometry dependence. They also reported that chair (zigzag-line) hydrogenated configuration is a direct (indirect) bandgap semiconductor. The authors highlight that the zigzag-line germanane could be used as a good optical linear polarizer due to highly anisotropic optical responses. In other theoretical study of germanane, Rivera−Julio *et al* [2] reported that the presence of various isomers in a mostly chair conformation material is expected due to the very small energy difference between the chair, z-line, and boat configurations. Sofo *et al* reported that graphane has two favorable conformations: a chair and boat geometry. Both of them present a direct bandgap at gamma point with 3.5 eV (3.7 eV) for the chair (boat) configuration [3].

The surface of 2D group III-V materials could be chemically modified by hydrogenation [4, 5, 9]. It has been found both theoretically and experimentally that hydrogen passivation stabilizes two dimensional buckled III-V sheets [10]. Recently, two-dimensional buckled gallium nitride was synthesized by hydrogen surface passivation and graphene encapsulation [10]. Chen *et al* reported that surface hydrogenation tunes the electronic and magnetic properties of 2D-BN [11]. Hydrogenization causes the 2D-BN sheet to have a smaller energy bandgap than the pristine one, while semihydrogenated BN is a ferromagnetic metal [12]. The configuration in which the hydrogen atoms are adsorbed on III-V devices plays an important role in their electronic properties. The fully hydrogenated 2D-BN prefers the zigzag-line configuration rather than the boat or chair configuration [13,14]. All three hydrogenated 2D-BN geometries: chair, zigzag-line and boat, are direct wide-bandgap semiconductors, where, their bandgap sizes are also hydrogen geometry dependent. The hydrogenation of 2D III-V materials could be of great interest not only to be stabilized and synthesized [10] but also to be used in a wide range of applications such as hydrogen storage, biosensors and bandgap tuning for manufacturing nanoelectronic devices [5].

Recently, 2D GaAs has been theoreti-

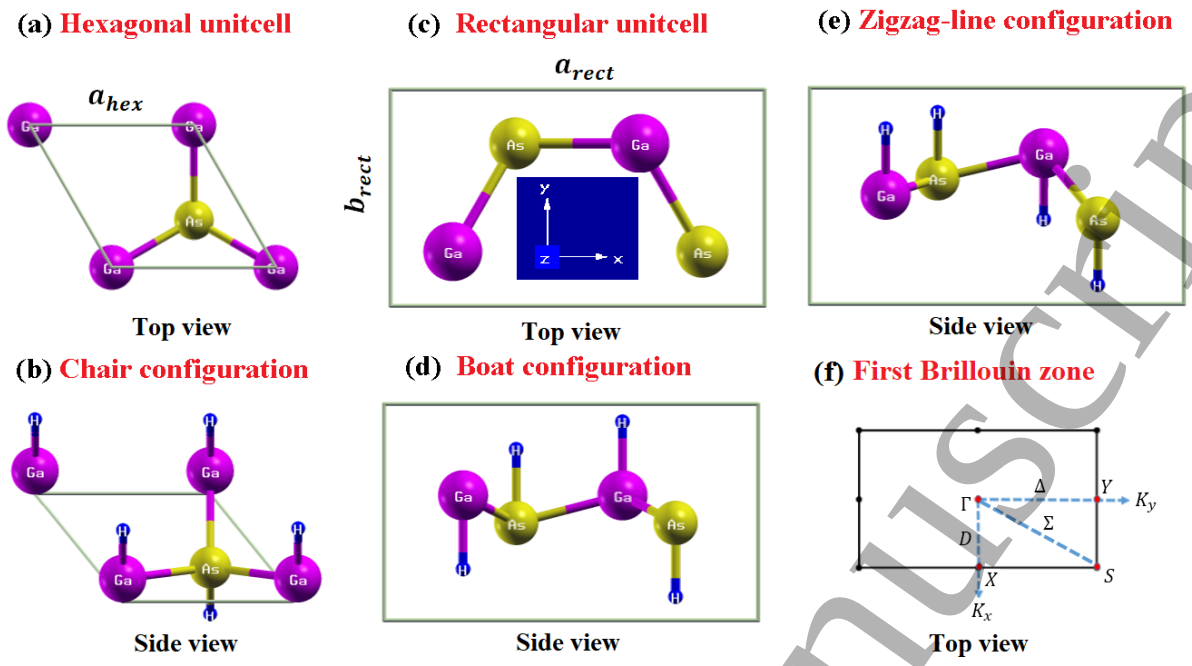

Figure 1. (Color online) Schematic representation for : (a) 2D-GaAs hexagonal unitcell (b) 2D H-GaAs chair configuration, (c) 2D H-GaAs rectangular unitcell (d) 2D H-GaAs boat configuration, (e) 2D H-GaAs zigzag-line configuration, and (f) high symmetry points in the Brillouin zone for the rectangular unitcell of 2D H-GaAs.

cally predicted to be a mechanically and dynamically stable semiconductor with buckled geometry not only in its pristine hexagonal unitcell but also forming a graphene-GaAs van der Waals heterostructure [15–17]. The authors also reported that electronic properties of GaAs and graphene can be modulated in a graphene-GaAs heterostructure [17]. In addition, some theoretical and experimental research highlight the importance of graphene/GaAs systems for future practical applications in plasmonic and photonic technology [18–22]. However, to the best of our knowledge, there are no previous studies about two-dimensional hydrogenated buckled GaAs system.

Although the dynamical stability of pristine 2D-GaAs has already been studied theoretically by first-principles calculations [15–17], this material has never been synthesized. The fact that some two-dimensional group III-V materials have been grown by functionalization with hydrogen passivation [10, 23, 24], motivated us to study the stability of two-dimensional hydrogenated buckled gallium arsenide. Thus, in order to explore a possible path towards the synthesis of 2D-GaAs, we have studied the dynamic stability of 2D-GaAs when it is functionalized with hydrogen. We have also determined the structural, mechanical and electronic properties of both materials to evaluate if hydrogen passivation improves these properties with respect to the pristine material. We will also contrast our results with other ab-initio theoretical studies of two-dimensional hydrogenated materials that have already been synthesized; indeed some of their physical properties are similar to those dis-

played by 2D-HGaAs, such as 2D-HBN and 2D-germanane. Finally, we will present potential applications for 2D-HGaAs taking into account the physical properties found in this study.

Therefore, the structural and electronic properties, as well as the energy and dynamical stability of 2D hydrogenated GaAs sheets will be studied in this work taking into account three different geometric configurations: chair, zigzag-line and boat using the Perdew-Burke-Ernzerhof functional (PBE) [25] within DFT framework [26, 27]. Furthermore, in order to study the effect of van der Waals interactions on energy stability, and both structural and electronic properties of 2D hydrogenated GaAs, long range electronic correlations will be treated by the Grimme's method (DFT−D2) [28].

2. Computational details

The calculations were performed using *vienna ab-initio simulation package* (VASP) [29, 30] employing the first principles projected augmented wave (PAW) method in the framework of the DFT [26, 27]. Exchange and correlation effects were treated with the generalized gradient approximation (GGA) implemented in the Perdew-Burke-Ernzerhof functional (PBE) [25]. Core electrons were described by the projector augmented wave (PAW) method [31, 32] wherein d states for Ga and As were included as valence electrons in their PAW pseudopotentials. The valence electron configurations for H, Ga and As are considered as $1s^1$, $3d^{10}4s^24p^1$ and $3d^{10}4s^24p^3$, respectively. The 2D-GaAs buckled hexagonal primitive cell, with one Ga atom and one As atom, see Figure 1(a), was constructed from the zinc-blende structure in the (111) plane [16]. The electron wave function was expanded in plane waves up to a cutoff energy of 500 eV for all the calculations. A gamma-centered grid of 25×25×1 k-point has been used to sample the irreducible Brillouin zone in the Monkhorst-Pack special scheme for calculations [33]. Phonon calculations have been performed by taking into account the interactions in a 8×8×1 2D H-GaAs supercell [34]. The PYPROCAR code was used to plot the electronic bands of 2D H-GaAs [35]. In addition, a 20 Å vacuum spacing between the adjacent supercells is kept to avoid interactions. For comparison, in order to study the effect of van der Waals interactions on energy stability, and both structural and electronic properties of 2D H−GaAs systems, calculations were also performed using Grimme's method (DFT−D2) [28]. To correct the bandgap values obtained by GGA-PBE and DFT-D2, hybrid functional Heyd-Scuseria-Ernzerhof (HSE) [36] band-calculations are carried out on the relaxed structures obtained with GGA-PBE and DFT-D2, respectively.

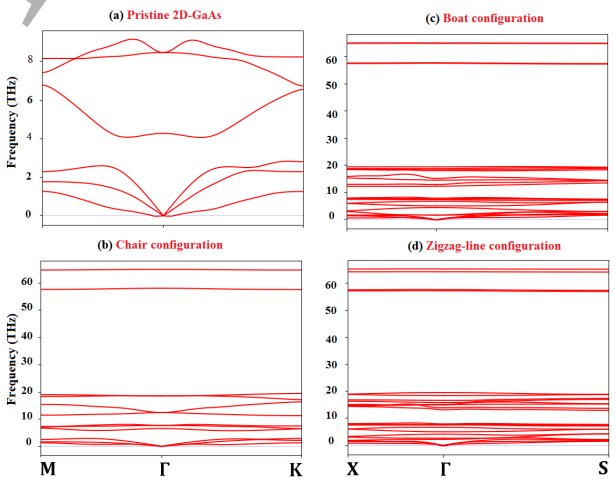

Figure 2. (Color online) Phonon dispersion curves for (a) pristine 2D-GaAs, (b) 2D H-GaAs chair configuration, (c) 2D H-GaAs boat configuration and (d) 2D H-GaAs zigzag-line configurations with DFT-PBE functional.

Table 1. Structural parameters for the pristine 2D-GaAs and three different configurations of 2D H-GaAs obtained by using PBE and vdW-Grimme method (DFT-D2) for comparison. The bandgap (E_g(eV)) was calculated with PBE and HSE functional. The adsorption (E_{ad}(eV/atom)) and formation (E_f(eV/atom)) energies were calculated with PBE functional and vdW-Grimme method (DFT-D2) for comparison.

	Hex-unitcell		Rect-unitcell		GaAsH-Configurations					
	Teo (Å)	*Teo vdW*(Å)	*Teo* (Å)	*Teo vdW*(Å)	*Chair* (Å)	*Chair vdW*(Å)	Boat (Å)	Boat *vdW*(Å)	Zigzag-line (Å)	Zigzag-line *vdW*(Å)
a_{hex}(Å)	4.05 3.97 [15] 4.05 [16]	4.00	–	–	4.08	4.01	–	–	–	–
a_{rect}(Å)	–	–	7.01	6.93	–	–	6.74	6.49	5.96	5.55
b_{rect}(Å)	–	–	4.04	4.00	–	–	4.06	3.99	4.06	3.99
d_{Ga-As}(Å)	2.41	2.39	2.41	2.39	2.48	2.45	2.49	2.46	2.48	2.45
d_{Ga-H}(Å)	–	–	–	–	1.56	1.56	1.56	1.56	1.56	1.55
d_{As-H}(eV)	–	–	–	–	1.52	1.51	1.52	1.51	1.52	1.51
buckling(Å)	0.58 0.55 [15] 0.58 [17]	0.60	0.51	0.60	0.79	0.80	0.88	0.92	0.86	0.86
$E_{g_{PBE}}$(eV)	1.09 ΓK 1.29 ΓK [15] 1.08 ΓK [16]	1.35 ΓK	–	–	1.68 ΓΓ	1.87 ΓΓ	2.16 ΓΓ	2.20 ΓΓ	2.23 ΓD	2.30 ΓD
$E_{g_{HSE}}$(eV)	1.89 ΓK	2.18 ΓK	–	–	2.51 ΓΓ	2.73 ΓΓ	2.98 ΓΓ	3.00 ΓΓ	3.19ΓD	3.32 ΓD
$E_{ad_{PBE}}$(eV/atom)	–	–	–	–	-1.180	-1.200	-1.179	-1.204	-1.182	-1.214
$E_{f_{PBE}}$(eV/atom)	–	–	–	–	-0.046	-0.066	-0.045	-0.070	-0.048	-0.080

Table 2. Bader charge state of Ga, As, H_{Ga} and H_{As} atoms in chair, boat and zigzag-line configurations for 2D H-GaAs systems with PBE and DFT-D2 functionals.

	Bader charge state			
	Pristine 2D-GaAs (e)	Chair (e)	Boat (e)	Zigzag-line (e)
Ga	+0.60	+0.84	+0.72	+0.70
vdW	+0.59	+0.84	+0.70	+0.67
As	−0.60	−0.21	−0.23	−0.20
vdW	−0.59	−0.20	−0.20	−0.16
H_{Ga}	–	−0.37	−0.32	−0.31
vdW	–	−0.37	−0.31	−0.31
H_{As}	–	−0.26	−0.17	−0.19
vdW	–	−0.26	−0.17	−0.19

3. Results and discussion

3.1. Energetic and dynamic stability

In order to study the 2D hydrogenated GaAs stability in the chair, boat and zigzag-line configurations, the adsorption energy was calculated. The adsorption energy is defined by:

$$E_{ad} = E_{H-GaAs} - E_{GaAs} - n_H E_H, \quad (1)$$

where E_{H-GaAs} and E_{GaAs} are the energies of the hydrogenated and pristine 2D-GaAs layers, n_H is the number of isolated spin-polarized hydrogen atoms, and E_H is the energy of a single isolated H atom. Table 1 displays these energies for comparison. The values obtained for chair, boat and zigzag-line configurations are -1.180 eV/atom (-1.200 eV/atom), -1.179 eV/atom (-1.204 eV/atom) and -1.182 eV/atom (-1.214 eV/atom), respectively, with PBE (DFT-D2) functional. We can see that all configurations are energetically stable with both PBE and DFT-D2 functionals. The adsorption energy value found for the chair geometry is of the same order of that reported for H-BN (-1.04 eV/atom) in the same geometry [12]. As H-BN chair configuration, the 2D hydrogenated GaAs presents an exothermic reaction and it could be obtained by the reaction of GaAs layers with H atoms. The zigzag-line configuration is energetically more favorable than the chair and the boat by 2 meV (14 meV) and 3 meV (4 meV), respectively, with PBE (DFT-D2) functional. These tiny energy differences with both PBE and DFT-

D2 indicate the metastability of 2D hydrogenated GaAs system. We can see that the adsorption energy is more negative with DFT-D2 when compared to that of PBE functional for each configuration by 20 meV (chair), 25 meV (boat) and 32 meV (zigzag-line). Using first principles density functional calculations, Bhattacharya *et al* reported that 2D hydrogenated BN prefers the zigzag-line configuration rather than the boat or chair configuration [13]. Tang *et al* found similar results for H-BN by dispersion-corrected density functional theory computations (DFT-D2) [14]. Regarding graphane, theoretical studies found that the chair configuration is the most stable one [7, 8, 37]. The energy stability order of our studied configurations was zigzag-line (zigzag-line), chair (boat) and boat (chair) with PBE (PBE-D2) functional. The reported energy stability order for H-BN and H-Ge was zigzag-line, boat and chair [2, 13, 14]. Authors also stated the metastability of these systems. For graphane, the reported configurations order was chair, zigzag-line and boat [37].

In order to compare the stability of H-GaAs with respect to other hydrogenated 2D systems, we calculated the 2D H-GaAs formation energies by the following mathematical expression:

$$E_f = E_{H-GaAs} - E_{GaAs} - n_H E_H^*, \qquad (2)$$

where E_{H-GaAs} and E_{GaAs} are the energies of the hydrogenated and pristine 2D-GaAs layers, n_H is the number of hydrogen atoms, and E_H^* is the energy of a H_2 molecule divided by two. From Table 1, the energy values obtained for the chair, boat and zigzag-line configurations are, respectively, -0.046 eV/atom (-0.066 eV/atom), -0.045 eV/atom (-0.070 eV/atom) and -0.048 eV/atom (-0.080 eV/atom) with PBE (DFT-D2) functional. The formation energies of our systems are negative, which physically means that hydrogenation of 2D-GaAs is feasible to occur. Sofo *et al* [3] reported a formation energy of -0.15 eV/atom and -0.10 eV/atom for graphane chair and boat configurations, respectively. Indeed, graphane has already been experimentally synthesized by various methods such as hydrogen plasma exposure of graphene, thermal exfoliation of graphene oxides, STM-assisted hydrogenation of graphene, plasma-enhanced CVD and electron-induced dissociation of HSQ on graphene [37, 38]. In addition, the fact that both thermal stability of hydrogenated boron nitride adsorbed on Ni(111) has been found experimentally [23, 24] and two-dimensional buckled gallium nitride has been synthesized by hydrogen surface passivation and graphene encapsulation on SiC(0001) [10], paves the way for the synthesis of other potential 2D group III−V materials such as buckled 2D-GaAs.

In order to study the dynamical stability of our systems, we have calculated the phonon dispersion at Γ point by a frozen phonon approach. Figure 2 displays the phonon dispersion curves for the pristine 2D-GaAs, and chair, boat and zigzag-line configurations with DFT-PBE functional. It proves stability of the studied system, since there are no imaginary frequencies in the phonon dispersion. Some negative frequencies near Γ point are visible as well. This feature has been found in other 2D-systems [39–43] and highlights the flexural acoustic mode of 2D-systems. They are often present in the theoretical calculations due to finite numerical and convergence accuracy close to Γ point [40]. The highest frequency modes, corresponding to H bond stretching modes, occur at 65.1 THz (2170 cm^{-1}) for the boat configuration, and at 64.8 THz (2160 cm^{-1}) and 64.7 THz (2157 cm^{-1}) for the chair and zigzag-line configurations, respectively. These results are

in accordance with those found for the energy stability of our systems. The vibrational frequency is lowest (highest) for the most (less) stable configuration. Therefore, the zigzag-line (boat) configuration has the highest (lowest) stability and the lowest (highest) mode of vibration. The reported highest frequency modes for graphane in the boat (3026 cm^{-1}) and chair (2919 cm^{-1}) configurations are higher than those reported in this work. This suggests a more covalent character for the H-C bond in graphane as compared to that of H-GaAs.

3.2. Structural properties

To study the structural properties of pristine 2D-GaAs, and compare them to those found for chair, boat and zigzag-line configurations, we have first optimized the structural parameters of 2D-GaAs hexagonal primitive cell. Then, from the obtained values, the 2D-GaAs rectangular unit cell has been constructed and relaxed (Figure 1(c)). The longer side length (a_{rect}) of this latter unit cell is three times the Ga-As shortest distance (d_{Ga-As}) of the hexagonal unit cell, while the other side (b_{rect}) is equal to the lattice parameter of the hexagonal primitive cell (a_{hex}). Finally, from these optimized hexagonal and rectangular unit cells, the chair (Figure 1(b)), and boat (Figure 1(d)) and zigzag-line (Figure 1(e)) configurations were built and relaxed, respectively.

The optimized parameters for 2D-GaAs monolayers: hexagonal and rectangular unit-cells, and chair, boat and zigzag-line configurations are depicted in Table 1. Our results for hexagonal 2D-GaAs unit cell are in good agreement with previous theoretical ones reported by DFT. Although the average Ga-As distance is almost the same for the three configurations, a slight difference in H atoms bonding of the chair, boat and zigzag-line configurations is found. Different from chair configuration, both boat and zigzag-line have two different GaAs bond lengths. In the former configuration, the GaAs distances are equal because all GaAs bonds connect with H atoms attached at opposite sides of the sheet. On the contrary, for both latter configurations, the length of the GaAs distance, where Ga and As bonding the H atoms lying on the opposite side of the plane, is shorter than those ones bonding the H atoms on the same side of the plane. For boat (zigzag-line) configuration the shortest Ga-As distance was 2.483 Å (2.483 Å); while the largest, due to H-H repulsion, was 2.493 Å (2.485 Å). Regarding to GaH and AsH bonds, we can see that, due to the charge repulsion, GaH bond lengths are larger than those of AsH in all three configurations. The GaH (AsH) bond lengths in all three configurations are almost the same, but higher than those found for BH (NH) in H-BN [13] and CH in graphane [3].

A comparison of structural results shows that both unit cell lattice parameters (hexagonal and rectangular) and cation-anion distance (d_{Ga-As} and d_{As-H}) decrease when we go from the DFT-D2 functional to PBE, while cation-cation distance (d_{Ga-H}) is the same for both functionals.

The average Ga-As distance (d_{Ga-As}) for chair, boat and zigzag-line configurations are larger than the one found for pristine 2D-GaAs by 2.90% (2.51%), 3.32% (2.93%) and 2.90% (2.51%), respectively, when using PBE (vdW) functional, as shown in Table 1. In order to get physical insight on the plasticity and stiffness of pristine 2D-GaAs when hydrogenated, the mechanical properties for hexagonal pristine 2D-GaAs and hexagonal 2D-HGaAs chair configuration are compared. We found that in-plane Young's modulus (Poisson's ratio) for pristine 2D-GaAs is higher (smaller) than that

of 2D-HGaAs chair configuration when using PBE functional by 125% (31.92%), which means that the pristine 2D-GaAs material displays less stiffness and more plasticity when hydrogenated. The values found for the in-plane Young's modulus (Poisson's ratio) for pristine 2D-GaAs and 2D-HGaAs materials are 44.4 Jm^{-2} (0.32) and 19.7 Jm^{-2} (0.47), respectively. The Poison's ratio ν and the in-plane Young's modulus Y are obtained from the calculated C_{11} and C_{12} elastic constants and multiplied later by the corresponding optimized unit-cell z distance. Their respective definitions are [44]:

$$\nu = C_{12}/C_{11} \tag{3}$$

$$Y = (C_{11}^2 - C_{12}^2)/C_{11} \tag{4}$$

3.3. Electronic structure and Bader charge transfer analysis

The electronic band structures for the pristine 2D-GaAs sheet, and chair, boat and zigzag-line configurations for 2D H-GaAs obtained with the PBE functional are displayed in Figure 3. The red lines represent the contributions of GaAs-4p_z orbitals, the black lines represent the contributions of GaAs-4p_{xy} mixed orbitals, while the yellow ones the contribution of either GaAs-4s (pristine 2D-GaAs) or GaAs-4s and H-1s mixed orbitals (2D H-GaAs). We can see in Figure 3(a), for the pristine 2D-GaAs sheet, that hybridized 4p_z and 4p_{xy} orbitals are near the Fermi level in the valence bands, and 4s and 4p mixed unoccupied orbitals, in the conduction bands. In addition, 4s orbital can be seen at the bottom of the conduction band. From band structures for the chair, boat and zigzag-line configurations (Figures 3(b), 3(c) and 3(d), respectively) we can see in the valence bands an increased overlapping between p_z and both planar p_{xy} and s orbitals

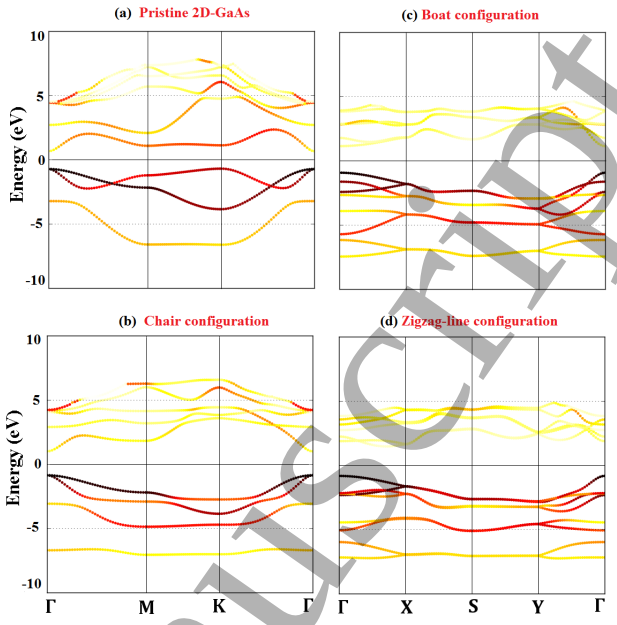

Figure 3. (Color online) Electronic band structure for (a) the pristine 2D-GaAs sheet, and (b) chair, (c) boat and (d) zigzag-line configurations for 2D H-GaAs, with DFT-PBE functional. The red lines represent the contributions of GaAs-4p_z orbitals, the black lines the contributions of GaAs-4p_{xy} mixed orbitals, and the yellow lines represent the contributions either the GaAs-4s orbitals (pristine 2D-GaAs) or GaAs-4s and H-1s mixed orbitals (2D H-GaAs).

when compared to the ones for pristine 2D-GaAs sheet (Figure 3(a)). As a result, the sp^2 hybridization becomes weaker, and the sp^3 one, stronger. Therefore, the average Ga-As atoms bond length (d_{Ga-As}) for all three configurations is much larger than that of pristine 2D-GaAs, as shown in Table 1. Furthermore, in comparison to pristine 2D-GaAs band structure, an extra s orbital, due to H contribution, is shown in the bottom of the valence bands for all three configurations.

From Figures 3(a), 3(d) and 1(f), we can see that pristine 2D-GaAs and zigzag-line configurations are Γ-K and Γ-D indirect semiconductors, respectively; while, from Figures 3(b) and 3(c), the Chair and boat

configurations display a Γ-Γ direct bandgap nature. As shown in Table 1, the corrected bandgap values for chair, boat and z-line configurations with HSE method are higher than those ones found by DFT-PBE (DFT-D2) for chair, boat and z-line, by 49.40% (46.00%), 37.96% (36.36%) and 43.05% (44.35%), respectively. The bandgap sizes of all studied configurations are also hydrogen dependent, and wider than that of pristine 2D-GaAs with PBE, PBE-vdW and HSE functionals, as shown in Table 1. Thus, the presence of H on 2D-GaAs layer opens the bandgap of 2D-GaAs layer, which makes it potential candidate for optoelectronic applications in the visible range. A qualitatively similar opening bandgap effect of H on graphene has been reported by Sofo *et al* [3]. On the contrary, hydrogenation causes 2D-BN sheet to have a smaller bandgap than the pristine one [12].

The bandgap energy for pristine 2D-GaAs changes from 1.89 eV (red light) to 2.51 eV (blue light), 2.98 eV (violet light), and 3.19 eV (violet light) for chair, boat, and zigzag configurations, respectively, with the HSE approach when hydrogenated. It can be noticed from Table 1 that hydrogen tunes the Γ-K indirect bandgap of pristine 2D-GaAs to Γ-Γ direct one for both chair and boat configurations, while the zigzag configuration remains indirect. Moreover, given that the energy differences for all three configurations are tiny, $\sim$ 2-3 meV with PBE functional, our results indicate that 2D-HGaAs is metastable in the chair, boat, and zigzag-line configurations, and thus the synthesis of these phases could be feasible by using the appropriate growth conditions and/or a specific substrate. Hence, the hydrogenation of 2D-GaAs tunes the bandgap of 2D-GaAs, which makes it a potential candidate for optoelectronic applications in the blue and violet ranges of the visible electromagnetic spectrum.

In order to get physical insight about the direction of charge transfer and ionicity of the studied 2D H-GaAs configurations, we have calculated the charge transference by Bader analysis [45]. For pristine 2D-GaAs a charge transfer of -0.60e (-0.59e) from Ga to As atoms with PBE (DFT-vdW) functional was found, as shown in Table 2. This charge transference is larger than that of -0.34e found in 2D H-BN [13], which means that our system is more ionic. For other configurations of H atoms, due to the charge conservation principle, the electron lost by the Ga atoms is gained by As, H_{Ga} and H_{As} atoms of the corresponding unit cell. For instance, we see in Table 2, for the chair configuration, a positive charge for Ga of +0.84e, while the net negative charge for As (-0.21e), H_{Ga} (-0.37e) and H_{As} (-0.26e) atoms is -0.84e.

The Bader analysis of Ga, As and H atoms in the three 2D H-GaAs configurations displays that in all configurations As, H_{As} and H_{Ga} acquire a negative charge state, gain electrons, while Ga acquires a positive charge state, looses electrons, as shown in Table 2. Physically, this takes place due to the electronegative difference between Ga, As and H atoms. We can also see that in all configurations the charge transference is higher than that of pristine 2D-GaAs sheet, which means that the ionicity increases. This result agrees with the increased sp^3 hybridization found in the band structure analysis for all configurations. The charge transference order found for our systems is chair > boat > zigzag-line. Table 2 also shows that the charge transference in all configurations is slightly minor with DFT-vdW when compared to that with PBE functional, but follow the

same qualitative trend. This effect cannot be directly attributed to van der Waals interactions since the DFT-D2 method is not self-consistent; rather, it is due to both the small change in atomic positions with respect to the ones obtained from PBE and the short range electronic interactions.

4. Conclusions

The ground state structure, stability, structural and electronic properties of two-dimensional hydrogenated GaAs with chair, boat and zigzag configurations have been studied by first-principles calculations with PBE and DFT-vdW functionals. To correct the bandgap values obtained by GGA-PBE, calculations with the hybrid functional Heyd-Scuseria-Ernzerhof (HSE) are carried out. The formation energy and phonon dispersion analysis display that all three hydrogenated configurations are stable semiconductors, where the most stable configuration is the zigzag, followed with a slight energy difference by chair (boat) and boat (chair) configurations with PBE (DFT-vdW) functional. Our results indicate that 2D-HGaAs is metastable in the chair, boat and zigzag-line configurations, and thus the synthesis of these phases could be feasible by using the appropriate growth conditions and/or a specific substrate. On the other hand, DFT-vdW interactions increase the adsorption energies and reduce the equilibrium distances when compared with PBE functional for the three configurations, but display qualitatively the same physical results on their stability and electronic properties. The calculated mechanical properties indicate that pristine 2D-GaAs displays less stiffness and more plasticity when it is hydrogenated. Electronic structures analysis shows that hydrogen reduces the in-plane sp^2 (σ bonding) hybridization, and increases the sp^3 hybridization when compared with pristine sheet. As a result, the 2D hydrogenated GaAs layers have a larger bandgap than the pristine one with both PBE and HSE functionals. In addition, zigzag is a $\Gamma-D$ indirect semiconductor, while chair and boat are $\Gamma-\Gamma$ direct semiconductors.

The bandgap energy for pristine 2D-GaAs changes from red to violet (blue) range for boat and zigzag (chair) configurations, with the HSE approach when hydrogenated. Our findings indicate that the presence of H on 2D-GaAs tunes the bandgap of pristine 2D-GaAs, which makes 2D-HGaAs a potential candidate for optoelectronic applications in the blue and violet ranges of the visible electromagnetic spectrum. Moreover, they suggest that 2D buckled-GaAs could be a good candidate to be synthesized by hydrogen surface passivation.

Conflicts of interest

There are no conflicts to declare.

Acknowledgements

This work has been carried out by the financial support of Universidad del Norte and Colciencias (Administrative Department of Science, Technology and Research of Colombia) under Convocatoria 712 - Convocatoria para proyectos de investigación en Ciencias Básicas, año 2015, Cod: 121571250192, Contrato 110-216. The authors gratefully acknowledge the support from the High Performance Computing core facility CalcUA and the TOPBOF project at the University of Antwerp, Belgium; and the computing time granted on the supercomputer Mogon at Johannes Gutenberg University Mainz (hpc.uni-mainz.de).

References

[1] DW Boukhvalov and MI Katsnelson. Chemical functionalization of graphene. *Journal of Physics: Condensed Matter*, 21(34):344205, 2009.

[2] J Rivera-Julio, A González-García, R González-Hernández, W López-Pérez, F M Peeters, and A D Hernández-Nieves. Vibrational properties of germanane and fluorinated germanene in the chair, boat, and zigzag-line configurations. *J. Phys.: Condens. Matter*, 31(075301):10pp, 2019.

[3] Jorge O Sofo, Ajay S Chaudhari, and Greg D Barber. Graphane: A two-dimensional hydrocarbon. *Physical Review B*, 75(15):153401, 2007.

[4] Huabing Shu, Yunhai Li, Shudong Wang, and Jinlan Wang. Quasi-particle energies and optical excitations of hydrogenated and fluorinated germanene. *Physical Chemistry Chemical Physics*, 17(6):4542–4550, 2015.

[5] Ying Ian Chen. *Nanotubes and nanosheets: functionalization and applications of boron nitride and other nanomaterials*. CRC Press, 2015.

[6] J-C Charlier, Xavier Gonze, and J-P Michenaud. First-principles study of graphite monofluoride (cf) n. *Physical Review B*, 47(24):16162, 1993.

[7] Marcel HF Sluiter and Yoshiyuki Kawazoe. Cluster expansion method for adsorption: Application to hydrogen chemisorption on graphene. *Physical Review B*, 68(8):085410, 2003.

[8] O Leenaerts, H Peelaers, AD Hernández-Nieves, B Partoens, and FM Peeters. First-principles investigation of graphene fluoride and graphane. *Physical Review B*, 82(19):195436, 2010.

[9] R González-Ariza, O Martínez-Castro, María G Moreno-Armenta, A Gonzalez-Garcia, W Lopez-Perez, and R Gonzalez-Hernandez. Tuning the electronic and magnetic properties of 2d g-gan by h adsorption: An ab-initio study. *Physica B: Condensed Matter*, 569:57–61, 2019.

[10] Zakaria Y Al Balushi, Ke Wang, Ram Krishna Ghosh, Rafael A Vilá, Sarah M Eichfeld, Joshua D Caldwell, Xiaoye Qin, Yu-Chuan Lin, Paul A DeSario, Greg Stone, et al. Two-dimensional gallium nitride realized via graphene encapsulation. *Nature materials*, 15(11):1166, 2016.

[11] Wei Chen, Yafei Li, Guangtao Yu, Chen-Zhong Li, Shengbai B Zhang, Zhen Zhou, and Zhongfang Chen. Hydrogenation: a simple approach to realize semiconductor- half-metal-metal transition in boron nitride nanoribbons. *Journal of the American Chemical Society*, 132(5):1699–1705, 2010.

[12] Yanli Wang. Electronic properties of two-dimensional hydrogenated and semihydrogenated hexagonal boron nitride sheets. *physica status solidi (RRL)–Rapid Research Letters*, 4(1-2):34–36, 2010.

[13] A Bhattacharya, S Bhattacharya, C Majumder, and GP Das. First principles prediction of the third conformer of hydrogenated bn sheet. *physica status solidi (RRL)–Rapid Research Letters*, 4(12):368–370, 2010.

[14] Qing Tang, Zhen Zhou, Panwen Shen, and Zhongfang Chen. Band gap engineering of bn sheets by interlayer dihydrogen bonding and electric field control. *ChemPhysChem*, 14(9):1787–1792, 2013.

[15] Hasan Şahin, Seymur Cahangirov, Mehmet Topsakal, E Bekaroglu, E Akturk, Ramazan Tuğrul Senger, and Salim Ciraci. Monolayer honeycomb structures of group-iv elements and iii-v binary compounds: First-principles calculations. *Physical Review B*, 80(15):155453, 2009.

[16] Alvaro Gonzalez-Garcia, William Lopez-Perez, Jagger Rivera-Julio, FM Peteers, Victor Mendoza-Estrada, and Rafael Gonzalez-Hernandez. Structural, mechanical and electronic properties of two-dimensional structure of iii-arsenide (1 1 1) binary compounds: An ab-initio study. *Computational Materials Science*, 144:285–293, 2018.

[17] Alvaro González-García, William López-Pérez, Rafael González-Hernández, Jairo Arbey Rodríguez, Milorad Milosevic, and Francois M Peeters. Tunable 2d-gallium arsenide and graphene bandgaps in graphene/gaas heterostructure: An ab-initio study. *Journal of Physics: Condensed Matter*, 2019.

[18] A Gamucci, D Spirito, M Carrega, B Karmakar, Antonio Lombardo, M Bruna, LN Pfeiffer, KW West, Andrea Carlo Ferrari, Marco Polini, et al. Anomalous low-temperature coulomb drag in graphene-gaas heterostructures. *Nature communications*, 5:5824, 2014.

[19] Shi-Sheng Lin, Zhi-Qian Wu, Xiao-Qiang Li, Yue-Jiao Zhang, Sheng-Jiao Zhang, Peng Wang, Rajapandiyan Panneerselvam, and Jian-

Feng Li. Stable 16.2% efficient surface plasmon-enhanced graphene/gaas heterostructure solar cell. *Advanced Energy Materials*, 6(21):1600822, 2016.

[20] Yanghua Lu, Sirui Feng, Zhiqian Wu, Yixiao Gao, Jingliang Yang, Yuejiao Zhang, Zhenzhen Hao, Jianfeng Li, Erping Li, Hongsheng Chen, et al. Broadband surface plasmon resonance enhanced self-powered graphene/gaas photodetector with ultrahigh detectivity. *Nano Energy*, 47:140–149, 2018.

[21] Nguyen Van Men and Nguyen Quoc Khanh. Plasmon modes in graphene–gaas heterostructures. *Physics letters A*, 381(44):3779–3784, 2017.

[22] Nguyen Van Men and Dong Thi Kim Phuong. Plasmon modes in bilayer-graphene–gaas heterostructures including layer-thickness and exchange-correlation effects. *International Journal of Modern Physics B*, 32(23):1850256, 2018.

[23] F Späth, J Gebhardt, F Düll, U Bauer, P Bachmann, C Gleichweit, A Görling, HP Steinrück, and C Papp. Hydrogenation and hydrogen intercalation of hexagonal boron nitride on ni (1 1 1): reactivity and electronic structure. *2D Materials*, 4(3):035026, 2017.

[24] Manabu Ohtomo, Yasushi Yamauchi, Xia Sun, Alex A Kuzubov, Natalia S Mikhaleva, Pavel V Avramov, Shiro Entani, Yoshihiro Matsumoto, Hiroshi Naramoto, and Seiji Sakai. Direct observation of site-selective hydrogenation and spin-polarization in hydrogenated hexagonal boron nitride on ni (111). *Nanoscale*, 9(6):2369–2375, 2017.

[25] John P Perdew, Kieron Burke, and Matthias Ernzerhof. Generalized gradient approximation made simple. *Physical review letters*, 77(18):3865, 1996.

[26] Pierre Hohenberg and Walter Kohn. Inhomogeneous electron gas. *Physical review*, 136(3B):B864, 1964.

[27] Walter Kohn and Lu Jeu Sham. Self-consistent equations including exchange and correlation effects. *Physical review*, 140(4A):A1133, 1965.

[28] Stefan Grimme. Semiempirical gga-type density functional constructed with a long-range dispersion correction. *Journal of computational chemistry*, 27(15):1787–1799, 2006.

[29] Georg Kresse and Jürgen Furthmüller. Efficiency of ab-initio total energy calculations for metals and semiconductors using a plane-wave basis set. *Computational materials science*, 6(1):15–50, 1996.

[30] Georg Kresse and Jürgen Furthmüller. Efficient iterative schemes for ab initio total-energy calculations using a plane-wave basis set. *Physical review B*, 54(16):11169, 1996.

[31] Peter E Blöchl. Projector augmented-wave method. *Physical review B*, 50(24):17953, 1994.

[32] Georg Kresse and D Joubert. From ultrasoft pseudopotentials to the projector augmented-wave method. *Physical Review B*, 59(3):1758, 1999.

[33] Hendrik J Monkhorst and James D Pack. Special points for brillouin-zone integrations. *Physical review B*, 13(12):5188, 1976.

[34] Atsushi Togo and Isao Tanaka. First principles phonon calculations in materials science. *Scripta Materialia*, 108:1–5, 2015.

[35] AH Romero and F Munoz. Pyprocar code, 2015.

[36] Jochen Heyd, Gustavo E Scuseria, and Matthias Ernzerhof. Hybrid functionals based on a screened coulomb potential. *The Journal of chemical physics*, 118(18):8207–8215, 2003.

[37] H Sahin, O Leenaerts, SK Singh, and FM Peeters. Graphane. *Wiley Interdisciplinary Reviews: Computational Molecular Science*, 5(3):255–272, 2015.

[38] Daniel C Elias, Rahul Raveendran Nair, TMG Mohiuddin, SV Morozov, P Blake, MP Halsall, Andrea Carlo Ferrari, DW Boukhvalov, MI Katsnelson, AK Geim, et al. Control of graphene's properties by reversible hydrogenation: evidence for graphane. *Science*, 323(5914):610–613, 2009.

[39] Qiang Wang and Dermot O'Hare. Recent advances in the synthesis and application of layered double hydroxide (ldh) nanosheets. *Chemical reviews*, 112(7):4124–4155, 2012.

[40] Sobhit Singh, Camilo Espejo, and Aldo H Romero. Structural, electronic, vibrational, and elastic properties of graphene/mos 2 bilayer heterostructures. *Physical Review B*, 98(15):155309, 2018.

[41] Sobhit Singh and Aldo H Romero. Giant tunable rashba spin splitting in a two-dimensional bisb monolayer and in bisb/aln heterostructures. *Physical Review B*, 95(16):165444, 2017.

[42] Weiyang Yu, Chun-Yao Niu, Zhili Zhu, Xiangfu Wang, and Wei-Bing Zhang. Atomically thin binary v–v compound semiconductor: a first-principles study. *Journal of Materials*

Chemistry C, 4(27):6581–6587, 2016.

[43] Hui Zheng, Xian-Bin Li, Nian-Ke Chen, Sheng-Yi Xie, Wei Quan Tian, Yuanping Chen, Hong Xia, SB Zhang, and Hong-Bo Sun. Monolayer ii-vi semiconductors: A first-principles prediction. *Physical Review B*, 92(11):115307, 2015.

[44] Richard Charles Andrew, Refilwe Edwin Mapasha, Aniekan M Ukpong, and Nithaya Chetty. Mechanical properties of graphene and boronitrene. *Physical review B*, 85(12):125428, 2012.

[45] Edward Sanville, Steven D Kenny, Roger Smith, and Graeme Henkelman. Improved grid-based algorithm for bader charge allocation. *Journal of computational chemistry*, 28(5):899–908, 2007.